

Electronic Supplementary Information (ESI)

Room Temperature Fabrication and Patterning of Highly Conductive Silver Features Using In-situ Reactive Inks by Microreactor-Assisted Printing

Chang-Ho Choi, Elizabeth Allan-Cole, Chih-Hung Chang*

Oregon Process Innovation Center/ Microproduct Breakthrough Institute and School of
Chemical, Biological & Environmental Engineering, Oregon State University, Corvallis,
Oregon 97331, United States

E-mail: Changch@che.orst.edu

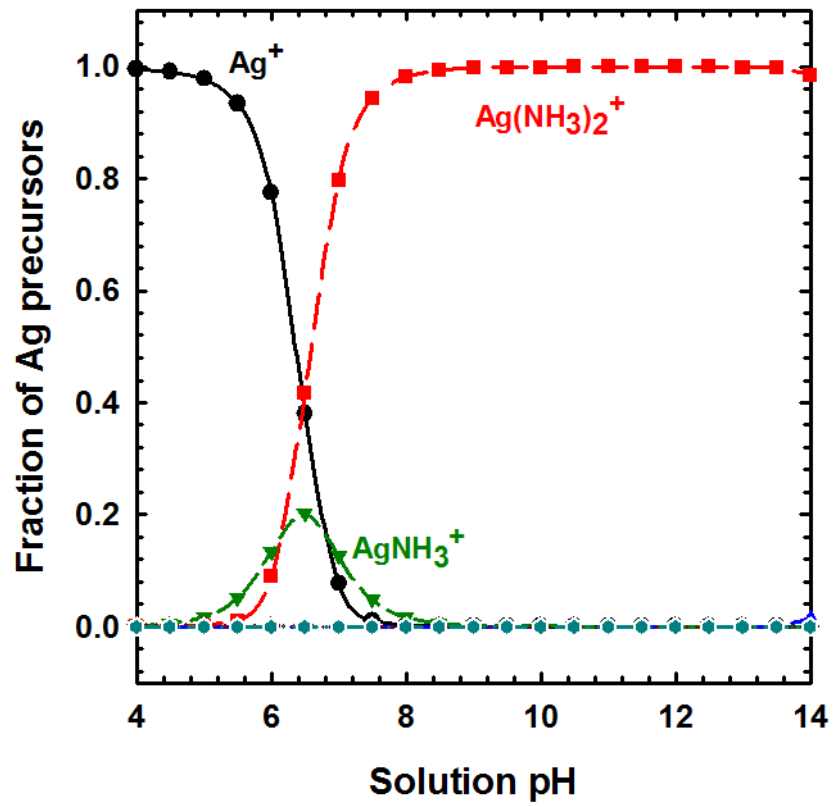


Fig. S1. Speciation diagram of silver precursors as a function of solution pH.
diagram of silver precursors as a function of solution pH.

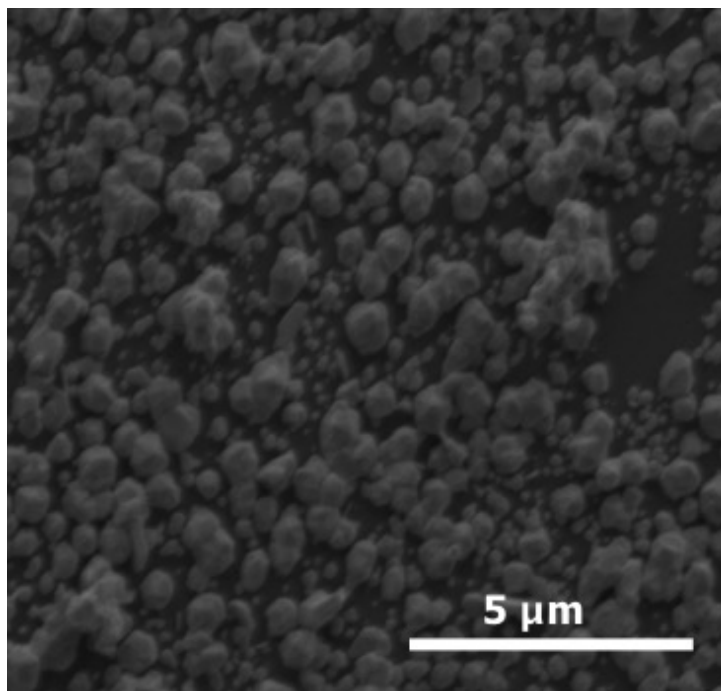


Fig. S2. Discontinuous silver film fabricated at a flow rate of 1.5 mL min^{-1} .

Silver film deposition

Fig. S2 shows the schematic diagram of the continuous flow microreactor deposition to fabricate the silver film. The deposition process consists of a microprocessor controlled dispensing pump (Ismatec), Tygon tubing (1.22 mm ID, Upchurch Scientific), and a micro T-mixer (Upchurch scientific). Silver nitrate (AgNO_3 , Alfa Aesar), ammonium hydroxide (30 vol % NH_4OH , Macron Chemicals), and Formaldehyde (36 vol % HCHO , Mallinckrodt Chemicals) were used as received without further purification. $\text{Ag}(\text{NH}_3)_2^+$ solution was prepared by mixing 7 mM AgNO_3 solution with 0.19 M ammonia solution. Deionized water was used as the solvent throughout the experiment. The $\text{Ag}(\text{NH}_3)_2^+$ solution was filtered by a filter paper (Whatman). A 5 mL HCHO solution was diluted with 50 mL deionized water. Prepared $\text{Ag}(\text{NH}_3)_2^+$ solution and formaldehyde (10 vol%) were initially pumped into the Tygon tubing. A micro-T-mixer allowed the homogeneous mixing of the reactants. Then, the mixture of the reactants passed through a 40 cm long linear reactor made by Tygon tubing. The reaction occurred at room temperature. A volumetric flow rate of 0.4 mL min^{-1} was employed. Silver ink solutions formed in the reactor were directly deposited on a soda lime glass substrate or a polyimide substrate sitting on a spin-coater under 1500 rpm, leading to uniform film formation. Both glass and polyimide substrates were treated with O_2 plasma prior to the deposition process for cleaning and promoting wettability of the substrates. After the O_2 plasma treatment, the contact angle of the bare glass substrate was reduced from 65° to 18° while the contact angle of 66° was reduced to 16° for the polyimide substrate.

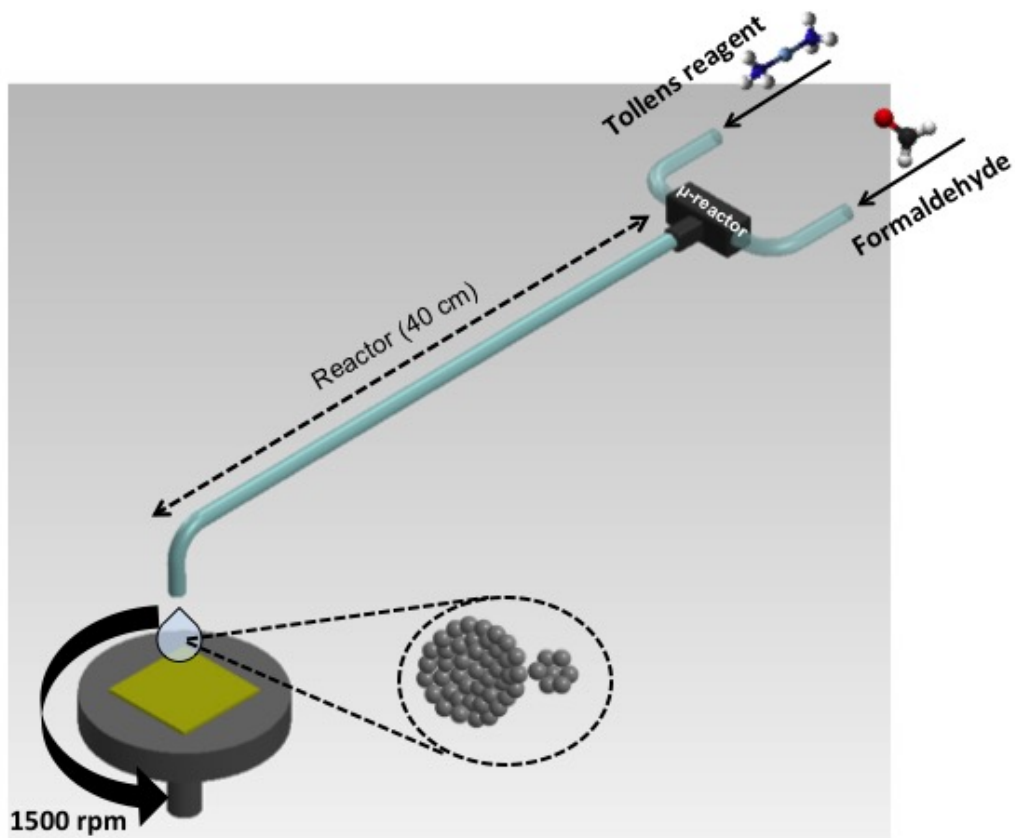


Fig. S3. Scheme of continuous flow microreactor deposition for silver film formation.

Silver line creation: Microchannel applicator was used to manufacture silver line. The Microchannel applicator consists of a transparent flow cell, microchannel, and gasket. Micro hot embossing technique was employed to prepare microchannel. The embosser was made by poly(methyl methacrylate) (PMMA). Embossing processes were divided into four distinct steps: 1) heating, 2) embossing, 3) cooling, and 4) demolding. A mold featured with the silver line dimension was first fabricated by photolithography technique. The mold then was used for the embossing process. The PMMA plate and mold were heated to 147 °C, followed by the embossing process where the mold was imprinted into the PMMA plate. The force for the embossing process was 500 N. After the embossing process, the mold and the imprinted embosser were cooled down to 90 °C. The embosser having same dimension as the mold was separated from the mold and used for the silver line patterning. Figure S3 describes the assembly of the microchannel applicator used to fabricate the silver line. The flow cell was made by polycarbonate, and thus the silver line formation can be visually observed throughout the deposition process. Gasket was installed to prevent leaking of the ink. Each component was stacked in the order as shown in the Figure. All components were tightly assembled by using clamps. Silver inks, synthesized in the microreactor, continuously flowed into the inlet port and guided to flow over the substrate by the microchannel. The deposition process was continued for 15 minutes to form the conductive silver line.

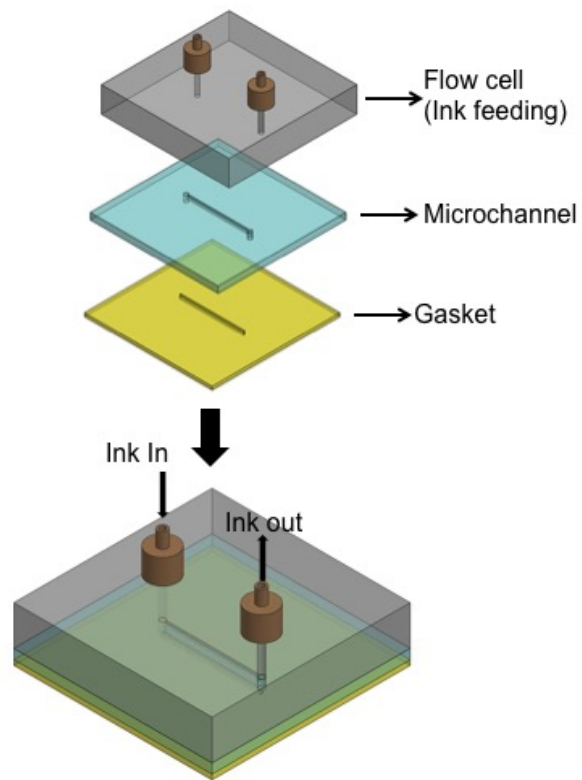


Fig. S4. Scheme of assembly of microchannel applicator

Characterizations of silver features

The morphologies and cross sectional areas of the silver films were examined by scanning electron microscopy (SEM, Quanta 600 FEG). The topography of the silver film was analyzed by atomic force microscopy (AFM, Veeco). Size and morphology of colloidal silver nanocrystals were analyzed using high resolution transmission electron microscopy (HRTEM). HRTEM images were taken by using a FEI Titan operated at 300 kV. The crystal phases of silver nanocrystals were analyzed by selected area electron diffraction (SAED). X-ray diffraction (XRD) was used to identify the crystallinity of silver film. XRD pattern was obtained by using a Rigaku Miniflex diffractometer with Cu K α radiation and a graphite monochromator. The conductivity of the film was obtained by using Hall-effect measurement with a Van der Pauw approach (Ecopia HMS-5000) at room temperature. In-situ optical properties of silver nanoink solutions were obtained by using an in-line UV-Vis absorption spectrophotometer (Ocean Optics Inc).

Table 1. Summary of reported silver film deposition

Deposition method	Sintering condition	Conductivity [S/m]
[27] Spray pyrolysis	350 °C (thermal)	1.4×10^7
[9] Printing reactive silver ink	150 °C (thermal)	8.8×10^6
[28] Printing silver NCs	200 °C (microwave sintering)	3.3×10^6
[29] Printing silver NCs	200 °C (thermal)	1.2×10^7
[30] Printing reactive silver ink	R.T	1.9×10^5
[31] Printing silver NCs	300 °C (thermal)	3.3×10^7
[32] Printing silver NCs	300 °C (thermal)	2.8×10^6
[33] Printing silver NCs	260 °C (thermal)	6.2×10^6
[34] Printing reactive silver ink	300 °C (thermal)	6.7×10^6
[35] Printing silver NCs	300 °C (thermal)	1.4×10^7
[36] Printing silver NCs	250 °C (thermal)	2.5×10^7
[37] Electroless deposition on Au NCs catalyst	R.T	1.6×10^7
[38] Spin coating silver NCs	250 °C (thermal)	4.2×10^6
[7] Printing silver NCs	550 °C (thermal)	1.0×10^7
[15] Printing reactive silver ink	90 °C (thermal)	6.2×10^7
[12] Printing silver NCs	R.T (HCl sintering)	1.0×10^7
[39] Laser E-beam to Ag precursors	R.T	1.0×10^5
[13] Printing silver NCs	110 °C (boiling water salt)	$\sim 3.3 \times 10^7$
[14] Silver-organic solution	> 150 °C	$\sim 6.2 \times 10^7$
This work	R.T	3.3×10^7

NCs: nanocrystals, R.T : room temperature

References

27. E. Zaleta-Alejandre, R. Balderas-Xicotencatl, M.L. Perez Arrieta, A.N. Meza-Rocha, Z. Rivera-Alvarez and C. Falcony, *Mater.Sci.Eng.,B*, 2013, **178**, 1147.
28. J. Perelaer, B.-J. de Gans and U. S. Schubert, *Adv. Mater.*, 2006, **18**, 2101.
29. T. H. J. van Osch, J. Perelaer, A. W. M. de Laat and U. S. Schubert, *Adv. Mater.* 2008, **20**, 343.
30. S. M. Bidoki, D. M. Lewis, M. Clark, A. Vakorov, P. A. Millner and D. McGorman, *J. Micromech. Microeng.*, 2007, **17**, 967.
31. S. B. Fuller, E. J. Wilhelm and J. M. Jacobson, *J. Microelectromech. Syst.* 2002, **11**, 54.
32. J. B. Szczech, C. M. Megaridis, D. R. Gamota and J. Zhang, *IEEE Trans. Electron. Packaging Manufact.*, 2002, **25**, 26.
33. H.-H. Lee, K.-S. Chou and K.-C. Huang, *Nanotechnology*, 2005, **16**, 2436.
34. Z. Liu and Y. Su, K. Varahramyan, *Thin Solid Films*, 2005, **16**, 2436.
35. J. Natsuki and T. Abe, *J. Colloid. Inteface. sci.*, 2011, **359**, 19.
36. S. Jeong, H. C. Song, W. W. Lee, Y. Choi and B.-H. Ryu, *J. Appl. Phys.*, 2010, **108**, 102805.
37. A. Inberg, P. Livshits, Z. Zalevsky, Y. Shacham-Diamand, *Micronelectron. Eng.*, 2012, **98**, 570.
38. K.-S. Chou, K.-C. Huang and H.-H. Lee, *Nanotechnology*, 2005, **16**, 779.
39. F. Stellacci, C. A. Bauer, T. Meyer-Friedrichsen, W. Wenseleers, V. Alain, S. M. Kuebler, S. J. K. Pond, S. R. Marder and J. W. Perry, *Adv. Mater.*, 2002, **14**, 194.